Publication I

Qinghong Jiang, Johanna Suomi, Markus Håkansson, Antti J. Niskanen, Miia Kotiranta, and Sakari Kulmala. 2005. Cathodic electrogenerated chemiluminescence of $Ru(bpy)_3^{2+}$ chelate at oxide-coated heavily doped silicon electrodes. Analytica Chimica Acta, volume 541, numbers 1-2, pages 159-165.

© 2004 Elsevier

Reprinted with permission from Elsevier.

Available online at www.sciencedirect.com
SCIENCE DIRECT®
Analytica Chimica Acta 541 (2005) 159–165
ANALYTICA CHIMICA ACTA
www.elsevier.com/locate/aca

Cathodic electrogenerated chemiluminescence of $Ru(bpy)_3^{2+}$ chelate at oxide-coated heavily doped silicon electrodes

Qinghong Jiang[a], Johanna Suomi[a], Markus Håkansson[a], Antti J. Niskanen[b], Miia Kotiranta[a], Sakari Kulmala[a,*]

[a] *Laboratory of Inorganic and Analytical Chemistry, Helsinki University of Technology, P.O. Box 6100, FIN-02015 HUT, Finland*
[b] *Microelectronics Center, Helsinki University of Technology, P.O. Box 3500, FIN-02015 HUT, Finland*

Received 16 June 2004; received in revised form 21 December 2004; accepted 21 December 2004
Available online 25 January 2005

Abstract

High amplitude cathodic pulse polarization of ultra thin oxide film-coated heavily doped silicon electrodes induces tunnel emission of hot electrons into aqueous electrolyte solution, which probably results in the generation of hydrated electrons in the vicinity of the electrode surface. The method allows the detection of tris (2,2′-bipyridine) ruthenium(II) chelate at subnanomolar concentration level. This paper shows that both n- and p-type heavily doped silicon electrodes can be used, illustrates the effect of oxide film thickness upon the silicon electrode on the intensity of ECL of tris (2,2′-bipyridine) ruthenium(II) and discusses the basic features of tris (2,2′-bipyridine) ruthenium(II) chelate-specific ECL at these electrodes. Thin oxide film-coated silicon electrodes provide a lower blank emission and a higher ECL intensity of the present ruthenium chelate than oxide-covered aluminium electrodes. This suggests that thin oxide film-coated silicon is a very promising working electrode material, especially in microanalytical systems made fully or partly of silicon.
© 2004 Elsevier B.V. All rights reserved.

Keywords: Electrogenerated chemiluminescence; Hot electrons; Ultra thin silicon dioxide films; Tunnel emission; $Ru(bpy)_3^{2+}$ chelate; Labels

1. Introduction

Metal/insulator/metal (M/I/M) and metal/insulator/electrolyte (M/I/E) tunnel junctions can act as cold cathodes and tunnel-emit hot electrons into aqueous medium [1–3]. It is essential that an aqueous medium can be used for some important analytical applications, for instance, immunoassays. The aqueous solution restricts the usable potential window to a quite narrow range when conventional active metal electrodes are used due to the hydrogen and oxygen evolution reactions. The use of semiconductor and thin insulating film-coated electrodes can widen the available potential window. The wider the obtainable potential window is, the more energetic light emissions are possible when chemiluminescence (CL) is produced.

Previous work showed briefly that $Ru(bpy)_3^{2+}$ chelates and Tb(III) chelates display strong electrogenerated chemiluminescence (ECL) in aqueous solutions at n-silicon electrodes oxidized in situ by anodic pulses during the measurement [4]. In the present work, we applied dry thermally grown silicon dioxide film-coated n- and p-type planar silicon discs as working electrodes [5] and studied further features of the ECL of $Ru(bpy)_3^{2+}$ chelate. A heavily doped n-silicon substrate has electron emission properties very similar [4,5] to aluminium metal used in the earlier studies [1,3] but the applicability of p-type silicon having quite a different work function was not obvious.

The insulating oxide film upon highly conducting silicon plays a key role in the present ECL: (i) it restricts ordinary cathodic reactions to occur below the onset electric field of tunnel emission process, (ii) it allows the silicon substrate to reach highly cathodic pulse potentials, (iii) it hinders the return of emitted electrons back to the substrate and (iv) it

* Corresponding author. Tel.: +358 9 4512601; fax: +358 9 462373.
E-mail address: sakari.kulmala@hut.fi (S. Kulmala).

0003-2670/$ – see front matter © 2004 Elsevier B.V. All rights reserved.
doi:10.1016/j.aca.2004.12.075

prevents substrate from quenching the excited states of luminophores.

Tris (2,2′-bipyridine) ruthenium(II), $Ru(bpy)_3^{2+}$, is one of the best-studied ECL-producing compounds [3,6,7]. Among other mechanisms, this chelate has been shown to produce ECL also during cathodic pulse polarization of oxide-covered aluminium electrodes in aqueous solutions [8] and it is in wide use as a label chelate in bioaffinity assays [3].

According to the previous studies, the cathodic chemiluminescence generation of $Ru(bpy)_3^{2+}$ in aqueous media is possible only in the simultaneous presence of strongly oxidizing species, such as, sulphate or hydroxyl radicals, and strongly reducing hot or hydrated electrons [8].

The aim of present work is to study the ECL of $Ru(bpy)_3^{2+}$ at heavily doped silicon electrodes in the presence of peroxydisulphate ions as sulphate radical's precursor, the effect of the thickness of the thermal oxide films and the analytical applicability of the present system.

2. Experimental

Antimony-doped n-Si(1 1 1) with resistivity of 0.008–0.015 Ω cm and boron-doped p-Si (1 0 0) with resistivity of 0.01–0.02 Ω cm were used as the electrode material. The insulating oxide films on the silicon wafers were fabricated by thermal oxidation in clean room. Firstly, the wafers were cleaned by standard RCA-cleaning process with HF-dip last. They were then oxidized immediately by thermal oxidation at 850 °C in 10% oxygen and 90% nitrogen atmosphere. Loading of the wafers into the furnace was at 700 °C in 5% oxygen and 95% nitrogen atmosphere, and temperature was ramped up 10 °C/min in the same atmosphere. After oxidation, the temperature was ramped down 4 °C/min in 100% nitrogen to 700 °C for unloading. The oxidation times varied for the various thickness of oxide film. Thickness of the oxide film was determined by an ellipsometer using the 632.8 nm wavelength (He–Ne laser). Because ultra thin silicon dioxide films give an erroneous refractive index during measurement, the refractive index of the SiO_2 was fixed as 1.465 known from thicker films and only the thickness was measured in our case. If the wafers were measured immediately after oxidation, and later the next day, the thickness increased about 0.05 nm due to adsorption of gases onto the surface. Silicon wafers were purchased from Okmetic Oy (Espoo, Finland), oxidized in the clean room and cut into 9.0 mm × 9.0 mm or 14.0 mm × 14.0 mm pieces to fit into the sample cell. The cell consisted of a sample holder made of Teflon and of a Pt-wire counter electrode (Fig. 1). The electrode effective area was normally 38.5 mm and 63.6 mm in special cases indicated in the text.

Measurements were mainly made in 0.05 mol dm^{-3} sodium tetraborate buffer at pH 9.2. The ECL intensity was measured by single photon counting with an apparatus that consisted of a Hamamatsu R 1527 photomultiplier, Stanford Research Systems SR-440 preamplifier, SR-400 gated photon counter in combination with Nucleus MCS-II scaler card attached in a PC computer. The MCS-II scaler card allowed time-resolved measurements and simultaneous measurements of light emitted during cathodic and intermittent zero voltage. Tris (2,2′-bipyridine) ruthenium(II) chloride hexahydrate, potassium peroxydisulfate and sodium tetraborate were p.a. products from Merck.

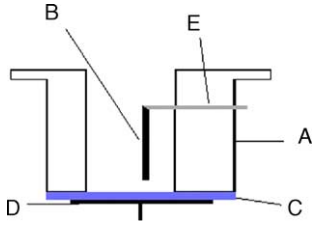

Fig. 1. Side view of ECL cell for measurements using silicon plate as working electrodes: (A) Teflon support; (B) Pt-counter electrode; (C) Al- or Si-plate working electrode; (D) working electrode contact; (E) counter electrode electrical contact wire.

3. Results and discussion

3.1. Basic features of $Ru(bpy)_3^{2+}$ ECL

$Ru(bpy)_3^{2+}$ shows typical ^{3}MLCT emission spectrum during cathodic pulse polarization at oxide-coated silicon or aluminium electrodes having the emission maximum at 620 nm [3,4,8]. Cathodic pulse polarization of thin insulating film-covered electrodes induces tunnel emission of hot electrons into aqueous electrolyte solution, as the primary step, which can lead to the formation of hydrated electrons after thermalization and solvation processes [1,2]. When hydrated electrons are available, sulphate radicals can be conveniently generated from peroxydisulphate ions [8,9]. After this initial process, the ECL excitation of $Ru(bpy)_3^{2+}$ can occur by the reduction-initiated oxidative excitation (red–ox) pathway or the oxidation-initiated reductive excitation (ox–red) pathway as discussed below.

Hot electron transfer through the insulating films occurs by tunnel emission in case of very thin films, or by Fowler–Nordheim tunnelling in case of thicker insulator films [2]. The simultaneous presence of oxidizing sulphate radical and hot or hydrated electrons is often a prerequisite to generate cathodic ECL in aqueous solution [2,3].

As quite an excellent one-electron oxidant, sulphate radical ($E^0 = 3.4$ V versus SHE [10]) is capable of oxidising aromatic compounds. This radical also has other excellent properties, e.g. it reacts very sluggishly with water [$k(SO_4^{\bullet -} + H_2O) = 60\ dm^3\ mol^{-1}\ s^{-1}$] [11]; its oxidizing power does not depend significantly on pH and it has only a weak tendency to addition and hydrogen absorption reaction. In the case of absence of reactive solutes, its decay is determined mainly by its self-combination rate [$k(SO_4^{\bullet -} + SO_4^{\bullet -}) = 8.1 \times 10^8\ dm^3\ mol^{-1}\ s^{-1}$] [11]. There-

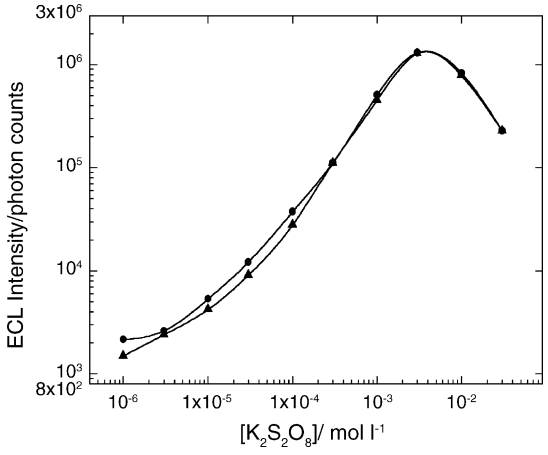

Fig. 2. Effect of $K_2S_2O_8$ concentration on $Ru(bpy)_3^{2+}$ chelate ECL. Conditions: 1.0×10^{-6} M $Ru(bpy)_3^{2+}$ in 0.05 M $Na_2B_4O_7$ at pH 9.2, coulostatic pulse generator, pulse charge 300 μC, voltage −25 V, frequency 50 Hz, (●) n^+-Si (thickness of oxide film 3.6 nm) and (▲) p^+-Si (thickness of oxide film 3.9 nm) as WE, respectively. ECL intensity was integrated over 1000 excitation cycles.

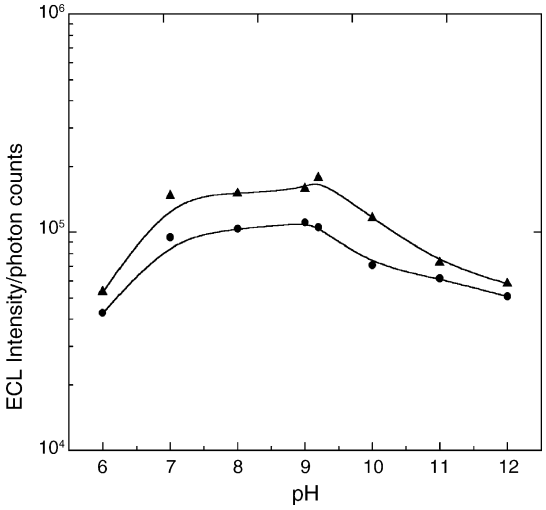

Fig. 3. Effect of pH on $Ru(bpy)_3^{2+}$ chelate ECL: (●) n^+-Si and (▲) p^+-Si. Conditions: 1.0×10^{-6} M $Ru(bpy)_3^{2+}$ in 0.1 M Na_2SO_4 and 30 mM $Na_2B_4O_7$ supporting electrolyte solution, 1.0×10^{-3} M $K_2S_2O_8$, solution was adjusted to the desired pH with sulfuric acid or sodium hydroxide, pulse charge 300 μC, pulse voltage −25 V and pulse frequency 50 Hz. ECL intensity was integrated over 1000 excitation cycles. Oxide film thicknesses as in Fig. 2.

fore, sulphate radical is often usable in generating or enhancing redox luminescence of chemiluminophores at thin insulating film-covered electrodes in aqueous solutions [2,3]. The dependence of the ECL intensity of $Ru(bpy)_3^{2+}$ on the concentration of peroxydisulphate ion concentration are presented in Fig. 2, both in the cases of n- and p-type silicon electrodes coated with ca. 4 nm thick thermal oxide film, which was known to be good insulating film thickness in case of aluminium oxide films and anodically oxidized silicon dioxide films [2,12].

At relatively low concentrations $K_2S_2O_8$ enhances the ECL intensity, however, the ECL intensity starts to decrease from 2×10^{-3} M $K_2S_2O_8$. The explanation is related to ECL mechanism. In principle, there are at least two obvious pathways to raise the $Ru(bpy)_3^{2+}$ to its excited states. The ECL excitation route of $Ru(bpy)_3^{2+}$ can occur by reduction-initiated oxidative excitation (red–ox) pathway (reactions (1a) and (1b)) or the oxidation-initiated reductive excitation (ox–red) pathway (reactions (2a) and (2b)) as follows [8]:

$$Ru(bpy)_3^{2+} + e_{aq}^- \rightarrow Ru(bpy)_3^{+} \quad (1a)$$

$$Ru(bpy)_3^{+} + SO_4^{\bullet -} \rightarrow Ru(bpy)_3^{2+*} + SO_4^{2-} \quad (1b)$$

$$Ru(bpy)_3^{2+} + SO_4^{\bullet -} \rightarrow Ru(bpy)_3^{3+} + SO_4^{2-} \quad (2a)$$

$$Ru(bpy)_3^{3+} + e_{aq}^- \rightarrow Ru(bpy)_3^{2+*} \quad (2b)$$

After these excitation steps, $Ru(bpy)_3^{2+*}$ relaxes (reaction (3)) to the ground state inducing the 620 nm peaking emission.

$$Ru(bpy)_3^{2+*} \rightarrow Ru(bpy)_3^{2+} + h\nu(620\,nm) \quad (3)$$

Due to the much shorter lifetime of the one-electron reduced form of the chelate in comparison to that of one-electron oxidized chelate, the ox–red pathway is probably the predominating excitation route [3,8]. In these excitation processes, at low concentration region, an increase of the concentration of $K_2S_2O_8$ increases the amount of the necessary reaction intermediates by reactions (1b) and (2a). At high concentrations ($>10^{-2}$ M), hydrated or hot electrons required for reactions (1a) and (2b) react too efficiently with the excess $K_2S_2O_8$, so that there are too low amount of reducing equivalents available in the system, which induces a decrease of ECL intensity. In the absence of peroxydisulfate ions, the source of oxidizing species is the reduction of dissolved molecular oxygen in one-electron steps and part of the excitation reactions can be based on the action of anion vacancies as discussed elsewhere [13,14].

The ECL intensity dependence of $Ru(bpy)_3^{2+}$ chelate on pH is presented in Fig. 3. The ECL intensity on oxide film-covered silicon electrodes seems to be quite constant in the slightly basic pH range. When H^+ acts as a hot or hydrate electron scavenger in acidic solutions, the ECL intensity decreases quite strongly. In alkaline region, ECL intensity also decreases considerably. We suggest that the decrease of ECL intensity must be based on the properties of the silicon dioxide film rather than on the effect of pH on the chelate itself. It is quite clear, that the present ultra thin silicon dioxide films can be dissolved and damaged in strongly basic solutions, and thus very alkaline solutions cannot be used.

When silicon and aluminum electrodes were compared, the ECL intensity of $Ru(bpy)_3^{2+}$ at oxide-coated silicon electrodes were found to be considerably higher than that observed at natural oxide film-covered aluminum under the same conditions inducing quite long-lasting cathodic pulses of the order of 2.2 ms. When pulse time was shortened by reducing the pulse charge of the coulostatic pulse generator, the difference between silicon and aluminum electrodes be-

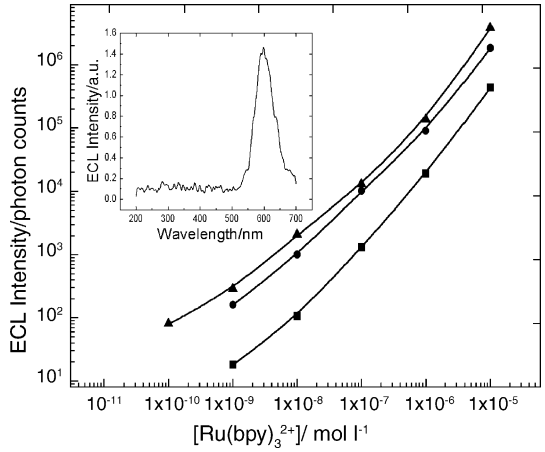

Fig. 4. Dependence of ECL intensity on $Ru(bpy)_3^{2+}$ concentration: (●) n^+-Si, (▲) p^+-Si and (■) aluminum with natural oxide film coverage when measurements were carried out on non-disposable basis. Conditions: 0.05 M $Na_2B_4O_7$ buffer at pH 9.2, 1.0×10^{-3} M $K_2S_2O_8$, $Ru(bpy)_3^{2+}$ chelate concentration varied, pulse charge 300 μC, pulse length ca. 850 μs, pulse voltage −25 V, pulse frequency 50 Hz and ECL intensity was integrated over 1000 excitation cycles. Blank and all the measurements in each series were carried out reusing the same working electrode disc. Oxide film thicknesses as in Fig. 2. Inset: uncorrected ECL spectrum of $Ru(bpy)_3^{2+}$ as measured by Perkin-Elmer LS-5 spectrometer.

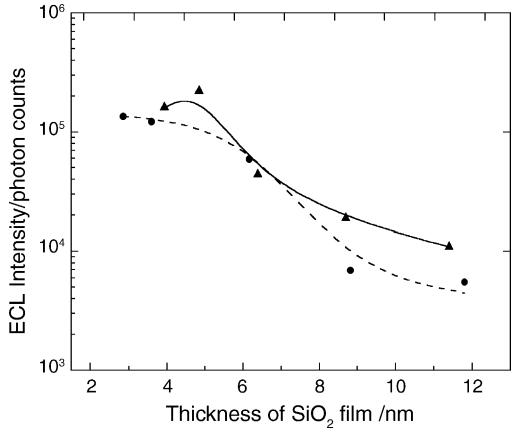

Fig. 5. Effect of oxide film thickness on ECL $Ru(bpy)_3^{2+}$: (●) n^+-Si and (▲) p^+-Si. Conditions: 0.05 M $Na_2B_4O_7$ buffer at pH 9.2, 1.0×10^{-3} M $K_2S_2O_8$, 1.0×10^{-6} M $Ru(bpy)_3^{2+}$, pulse charge 480 μC, voltage −50 V and frequency 50 Hz.

came smaller. The ECL intensity of p-type silicon electrodes seemed to be slightly better than that of n-type electrodes (Fig. 4). Thus, it is possible that a thermal oxidation of heavily doped p-type silicon might give a bit better quality oxide films under the used oxidation conditions.

3.2. The effect of oxide film thickness on the ECL intensity at oxide-covered silicon electrodes

Fig. 5 displays the effects of oxide film thickness on the ECL intensities of $Ru(bpy)_3^{2+}$ at heavily doped n- and p-type silicon electrodes, respectively. In both of cases, the ECL intensity started to decrease exponentially as the oxide film thickness exceeded 4–5 nm. Natural oxide films formed at room temperature on the present silicon electrodes are too thin to be usable according to the present excitation method unlike the natural oxide films formed upon aluminium at room temperature.

The effect of SiO_2 film thickness on the ECL intensity is quite similar to that of Al_2O_3 film thickness observed previously [2,14]. Thus, this supports the theory presented in the earlier papers [2,12,14]. The explanation is related to mechanism of hot electron tunnel emission during cathodic pulse polarization. A schematic representation of the tunnel emission of hot electrons into electrolyte solution during strong cathodic pulse polarization of the oxide-coated n-silicon working electrode has been presented earlier [4] and has been modified here to correspond to p-type silicon electrodes (Fig. 6).

The electrons tunnel through thin insulator film (<4–5 nm) ballistically or near ballistically so that no considerable loss of energy of electrons occurs (denoted as hot e^- type I

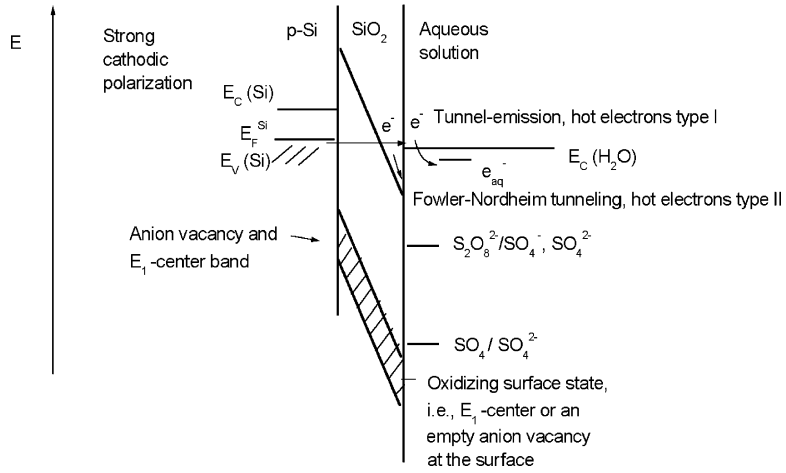

Fig. 6. Schematic diagram of tunnel emission of hot electrons from oxide-coated strongly doped p-type silicon.

Table 1
Comparison of ECL characteristics on different oxide-coated electrodes

Electrode	Blank signal intensity	ECL emission decay	ECL lag time (μs)	Rise time to reach 90% of ECL intensity (μs)
Aluminium	Highest	Longer	14	30
n^+-Silicon	Lowest	Short and identical to each other	8	
p^+-Silicon	Moderate			

in Fig. 6). However, with considerably thicker oxide films, Fowler–Nordheim tunnelling predominates as an electron transportation mechanism. In FN tunnelling regime, the electrons are transferred into the solution from the bottom of the conduction band of the insulator (denoted as hot e^- type II) or somewhat above the conduction band edge of oxide at the oxide/electrolyte solution interface due to the gaining of energy in the electric field while travelling in the conduction band [15–18]. In practice, the conduction band edge of SiO_2 at oxide/electrolyte solution interface bends down well below the conduction band edge of water due to the cathodic polarization [4]. However, the hydrated electrons can be generated only when hot electrons are injected into the conduction band of water. Hence, with thicker oxide films, hydrated electrons cannot be generated and the electrons transferred to solution species are not sufficiently energetic to induce efficient ECL.

Thermal oxidation is probably one of the simplest ways to grow an insulating oxide film on a silicon substrate. Thermally grown SiO_2 is an excellent insulator and the Si/SiO_2 interface formed by thermal oxidation is usually grown with a high degree of control regarding interface traps and fixed charge [19]. These features make thermally grown silicon dioxide films have potential in application of lab-on-chip or in micro-total analysis systems (μTAS) as one of commonly utilized material.

3.3. Analytical applicability and time-resolved ECL detection

We made some comparison of the ECL at oxide-coated heavily doped silicon electrodes and at aluminium electrode. The main characteristics are given in Table 1. It was first found out that oxide-covered aluminium electrodes showed much higher blank emission at this wavelength range and that thermal silicon oxide film formed on n-type silicon showed the lowest blank emission of all the electrode types tested (Fig. 7). Therefore, it is concluded that oxide films formed on n-type substrate possibly have less defects or impurities able to act as solid state electroluminescence emission centers under high field conditions in the oxide film which are necessary to achieve the tunnel emission of electrons into the electrolyte solution.

Thus, a calibration plot for $Ru(bpy)_3^{2+}$ was measured again using oxide-coated n-type electrode on disposable basis and with a slightly higher working electrode effective area (Fig. 8). Also the time-resolved signal was recorded for 200 μs right after the excitation pulses. However, the ^{3}MLCT excited state of $Ru(bpy)_3^{2+}$ has so short luminescence lifetime that time-resolved ECL signal is probably not very usable. Interestingly, the present ECL has a considerably longer-lasting emission on oxide-covered aluminium electrodes than at silicon electrodes which might allow the use of TR-ECL signal in a case of simultaneous use of a

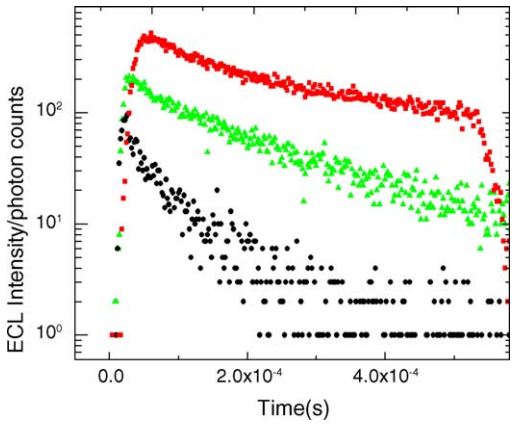

Fig. 7. ECL blank emission pulses at 620 nm: (●) n-silicon with 3.6 nm oxide film, (▲) p-silicon with 3.7 nm oxide film and (■) aluminium with natural oxide film. Conditions: as in Fig. 4.

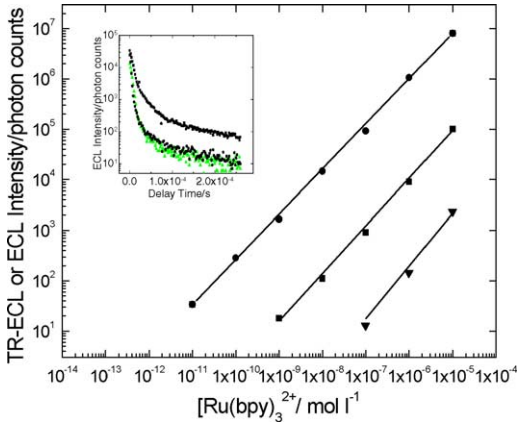

Fig. 8. Calibration curve for $Ru(bpy)_3^{2+}$ using disposable electrodes and either cathodic signal or time-resolved signal after the excitation pulse: (●) cathodic ECL at disposable n-silicon electrodes with 3.6 nm thermal oxide film coating, (▼) time-resolved signal at oxide-coated n-silicon electrodes and (■) time-resolved signal using disposable oxide-covered aluminium electrodes. Conditions: electrode area 63.6 mm^2, 0.05 M $Na_2B_4O_7$ buffer at pH 9.2, 3.0×10^{-3} M $K_2S_2O_8$, pulse charge 120 μC, pulse length ca. 560 μs, pulse voltage −45 V and pulse frequency 20 Hz. Time-resolved measurements: delay time 0 μs and gate time 200 μs. ECL intensity was integrated over 1000 excitation cycles. Inset: decay of ECL at 620 nm at n-silicon electrode ((●) 3.6 nm oxide film), p-silicon electrode ((▲) 3.7 nm oxide film) and natural oxide-covered aluminum electrode ((■) ca. 2 nm oxide film).

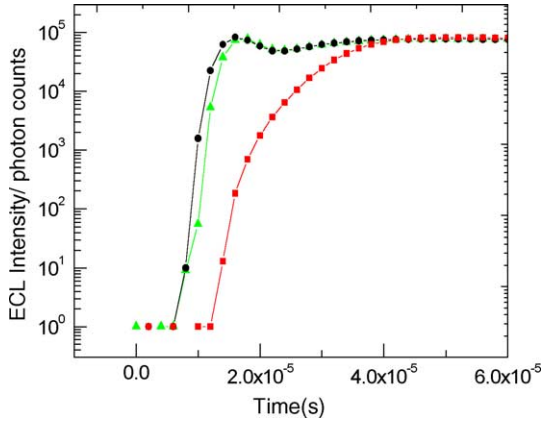

Fig. 9. The rise of the ECL pulse at different electrode types: (●) n-silicon with 3.6 nm oxide film, (▲) p-silicon with 3.7 nm oxide film and (■) aluminium covered with a natural oxide film. Conditions: as in Fig. 8 except ECL integrated over 5000 excitation cycles.

$Ru(bpy)_3^{2+}$-based label together with, e.g. coumarine labels, which display no ECL after the excitation pulse.

The decay of 1×10^{-5} M $Ru(bpy)_3^{2+}$ solution was separately studied integrating ECL over 5000 excitation cycles (inset of Fig. 8). It was observed that the ECL at oxide-coated n- and p-type silicon had identical and much faster decays than that observed at oxide-covered aluminum. The decay at oxide-covered aluminum electrode could be divided into three separate exponential processes with luminescence lifetimes of 6.8, 43 and 95 μs, which, however, we cannot address to certain specific chemical processes. We believe that an explanation for this phenomenon is that for some reason some of the radical species generated at the surface of aluminum oxide film have a somewhat longer lifetime than in the vicinity of silicon dioxide film. Another explanation might be, that electrode surface alkalization due to hydrogen evolution reaction [2] could thin the oxide film so much during the cathodic excitation pulse that electron transfer by tunneling through the oxide film becomes possible also in the absence of the electric field across the oxide film induced by the external voltage source. Thus, this "long-lived ECL" would be just CL induced by metallic aluminum metal behaving as a strong reducing agent. When the oxide film has sufficiently grown a bit thicker charge transfer through the oxide film becomes again impossible and the luminescence disappears.

The rise of the ECL signal was also studied under the present ECL conditions. Fig. 9 shows the growth of the present ECL pulses at oxide-covered Al and Si electrodes. The present ultra thin oxide film-coated n- and p-type silicon electrodes have a lag time about 8 μs from the onset of voltage, and a current pulse before any luminescence is observed. The lag time is a bit longer for aluminium oxide film, i.e. about 14 μs (Fig. 9). However, in all of the present cases the rise time from the moment of zero intensity to 90% intensity is about 30 μs. Presently, we cannot give an explanation to the different lag times between silicon dioxide and aluminum oxide film, which is however, reproducibly observed always.

4. Conclusions

Cathodic pulse polarization of oxide-coated heavily doped silicon induces strong ECL of $Ru(bpy)_3^{2+}$ chelate and both n- and p-type silicons are usable as an electrode material. The optimal thermal silicon dioxide film thickness is around 2–5 nm. The calibration curves of $Ru(bpy)_3^{2+}$ chelate in various conditions span over many orders of magnitude of concentration allowing very low detection limits. The presence of sulphate radicals enhances $Ru(bpy)_3^{2+}$ ECL intensity strongly and the optimal peroxodisulfate ion concentration as a coreactant is ca. 3×10^{-3} mol/l when the pulse charge is around 300 μC. The ECL intensity has a maximum at neutral or slightly basic pH range. Borate buffer at pH 9.2 is an excellent supporting electrolyte for the generation of the present ECL.

Good sensitivity of this ECL method makes it promising to apply disposable oxide-coated silicon electrodes as a solid phase for immunoassays or other probing assays, especially in miniaturized assay formats using $Ru(bpy)_3^{2+}$-based labels available commercially. $Ru(bpy)_3^{2+}$-based labels combined with other electrochemiluminescent labels with a longer luminescence lifetime can also provide multicomponent assays by application of wavelength and/or time discrimination. As a detection technique, ECL has a lot of potential for applications in miniaturized analysis, and in devices fabricated using highly sophisticated silicon technology of the present day easily available in most of the industrialized countries.

References

[1] S. Kulmala, K. Haapakka, J. Alloys Compd. 225 (1995) 502.
[2] S. Kulmala, T. Ala-Kleme, L. Heikkilä, L. Väre, J. Chem. Soc., Faraday Trans. 93 (1997) 3107.
[3] S. Kulmala, J. Suomi, Anal. Chim. Acta 500 (2003) 21, and references cited therein.
[4] T. Ala-Kleme, S. Kulmala, M. Latva, Acta Chem. Scand. 51 (1997) 541.
[5] M. Helin, L. Väre, M. Hakansson, P. Canty, H.-P. Hedman, L. Heikkilä, T. Ala-Kleme, J. Kankare, S. Kulmala, J. Electroanal. Chem. 524–525 (2002) 176.
[6] K.A. Fähnrich, M. Pravda, G.G. Guilbault, Talanta 54 (2001) 551.
[7] R.D. Gerardi, N.W. Barnett, S.W. Lewis, Anal. Chim. Acta 378 (1999) 1, and references cited therein.
[8] T. Ala-Kleme, S. Kulmala, L. Väre, M. Helin, Anal. Chem. 71 (1999) 5538.
[9] S. Kulmala, A. Hakanen, P. Raerinne, A. Kulmala, K. Haapakka, Anal. Chim. Acta 309 (1995) 197.
[10] R. Memming, J. Electrochem. Soc. 116 (1969) 785.
[11] P. Neta, R. Huie, A. Ross, J. Phys. Chem. Ref. Data 17 (1988) 1027.
[12] S. Kulmala, T. Ala-Kleme, H. Joela, A. Kulmala, J. Radioanal. Nucl. Chem. 232 (1998) 91.

[13] S. Kulmala, A. Kulmala, M. Helin, I. Hyppänen, Anal. Chim. Acta 359 (1998) 71.
[14] S. Kulmala, A. Kulmala, T. Ala-Kleme, J. Pihlaja, Anal. Chim. Acta 367 (1998) 17.
[15] D. Dimaria, E. Cartier, J. Appl. Phys. 78 (1995) 3883.
[16] D. Arnold, E. Cartier, D. DiMaria, Phys. Rev. B 49 (1994) 10278.
[17] D. DiMaria, M. Fischetti, J. Appl. Phys. 64 (1988) 4683.
[18] E. Cartier, D. DiMaria, J. Appl. Phys. 78 (1995) 3883.
[19] A.R. Barron, Adv. Mater. Opt. Electron. 6 (1996) 101.